J Biomol NMR (2008) 41:9–15
DOI 10.1007/s10858-008-9233-7

ARTICLE

Resolution enhancement by homonuclear J-decoupling: application to three-dimensional solid-state magic angle spinning NMR spectroscopy

Lichi Shi · Xiaohu Peng · Mumdooh A. M. Ahmed · Dale Edwards · Leonid S. Brown · Vladimir Ladizhansky

Received: 21 January 2008 / Accepted: 20 March 2008 / Published online: 11 April 2008

Abstract We describe a simple protocol to achieve homonuclear J-decoupling in the indirect dimensions of multidimensional experiments, and to enhance spectral resolution of the backbone Cα carbons in the 3D NCACX experiment. In the proposed protocol, the refocusing of the Cα–CO homonuclear J-couplings is achieved by applying an off-resonance selective π pulse to the CO spectral region in the middle of Cα chemical shift evolution. As is commonly used in solution NMR, a compensatory echo period is used to refocus the unwanted chemical shift evolution of Cα spins, which takes place during the off-resonance selective pulse. The experiments were carried out on the β1 immunoglobulin binding domain of protein G (GB1). In GB1, such implementation results in significantly reduced line widths, and leads to an overall sensitivity enhancement.

Keywords Solid-state NMR · Magic angle spinning · Uniformly ^{13}C,^{15}N labeled proteins · Assignments · Homonuclear decoupling · Resolution enhancement

Abbreviations

SSNMR	Solid-state NMR
MAS	Magic angle spinning
GB1	β1 immunoglobulin binding domain of protein G
TPPI	Time proportional phase increment
SPINAL64	Small phase incremental alternation with 64 steps
DSS	2,2-Dimethyl-2-silapentane-5-sulfonic acid

Electronic supplementary material The online version of this article (doi:10.1007/s10858-008-9233-7) contains supplementary material, which is available to authorized users.

L. Shi · X. Peng · M. A. M. Ahmed · D. Edwards · L. S. Brown · V. Ladizhansky (✉)
Department of Physics and Biophysics Interdepartmental Group, University of Guelph, 50 Stone Road East, Guelph, ON, Canada N1G 2W1
e-mail: vladimir@physics.uoguelph.ca

Introduction

High spectral resolution and sensitivity are prerequisites for the successful structural NMR studies of proteins. In magic angle spinning (MAS) solid-state NMR (SSNMR) experiments, ^{13}C and ^{15}N are usually the nuclei of choice for detection, and the width of ^{13}C resonance lines is one of the major determinants of spectral resolution. The spectral resolution is especially critical for samples with a uniform incorporation of ^{13}C and ^{15}N labels, which are required for a complete high-resolution structure determination. In recent years, a number of protocols have been developed that yield structurally homogeneous samples of soluble proteins in microcrystalline form (Pauli et al. 2000; Martin et al. 2003), amyloid fibrils (Jaroniec et al. 2002; Siemer et al. 2005; Paravastu et al. 2006), and membrane proteins (Hiller et al. 2005; Lorch et al. 2005). In such samples, the inhomogeneous line broadening resulting from structural heterogeneity is minimized. Contributions to the line shapes (Duma et al. 2003c; Igumenova et al. 2003) and to the values of isotropic shifts (Wylie et al. 2008) of ^{13}C resonances in uniformly ^{13}C-labeled proteins were recently examined by various groups. It was found that at moderate spinning frequencies around 85 ppm for ^{13}C, when the isotropic line positions are the least affected (Wylie et al. 2008) by the residual rotational resonance effects (Andrew et al. 1963; Levitt et al. 1990), the line shapes of the CO and Cα resonances are an interplay

between J-couplings, homonuclear dipolar interactions, and chemical shift anisotropy effects. Removal of some of these contributions would help reduce the observed line width, and improve spectral resolution. Accordingly, various groups have recently discussed how homonuclear J-decoupling can be implemented in MAS SSNMR. In particular, J-decoupling in the indirect dimensions of multidimensional experiments has been demonstrated to result in resolution enhancement (Straus et al. 1996, 1998; Igumenova et al. 2005; Zhou et al. 2006) in SSNMR spectra. In most cases, it has relied upon the combination of soft and hard π-pulses (Bruschweiler et al. 1988) applied on-resonance in the middle of the indirect chemical shift evolution period. Straus et al. (1996, 1998) demonstrated that this approach results in significant spectral resolution enhancement for backbone carbon resonances in 2D and 3D MAS SSNMR spectra. Constant time evolution and off-resonance selective pulses were recently used in the context of J-MAS spectroscopy (Chen et al. 2007; Zhong et al. 2007), and were also shown to result in significant resolution enhancements in protein spectra. Alternatively, Duma et al. (2003a, b) showed that J-couplings can be removed through the application of "In-Phase-Anti-Phase" technique. More recently, Chevelkov et al. (2005) demonstrated the use of selective pulses for J-decoupling in the direct dimension during acquisition.

Resolution enhancement for Cα resonances is the focal point of this work. While the soft–hard pulse pair works well for carbonyls, it is harder to achieve homogeneous refocusing for Cα spins because of relatively large chemical shift dispersion of the resonances. Thus, although the soft–hard pulse pair allows refocusing both Cα–CO and Cα–Cβ J-couplings simultaneously, the practical implementation may not be so straightforward, especially at high magnetic fields. Recently, Rienstra and co-workers have presented a comprehensive analysis and optimization of the selective pulses under MAS conditions (Li et al. 2006), and could achieve more homogeneous inversion band-widths, albeit some signal losses were observed.

An alternative approach inspired by solution NMR techniques, and demonstrated in this work in the context of dipolar-mediated MAS chemical shift correlation experiments, is to apply $J_{COC\alpha}$-refocusing pulse off-resonance to the carbonyl region. The advantages are clear: carbonyl resonances are well separated and one can achieve homogeneous $J_{COC\alpha}$ refocusing with short selective pulses and without affecting aliphatic spins, thus minimizing the relaxation losses. We demonstrate how this can be implemented in the context of the 2D ^{13}Cα–^{15}N and 3D ^{15}N–^{13}Cα–^{13}Cx chemical shift correlation experiments. Despite the fact that only Cα–CO J-interactions are refocused, significant resolution enhancements were achieved for Cα lines in the indirect dimension.

Materials and methods

Sample preparation

A 6.2 kDa, 56 residue protein, β1 immunoglobulin binding domain of protein G (GB1) was used in the experiments. The T2Q mutant of GB1 was heterologously expressed in *E. coli* BL21 (DE3) grown in minimal media (1 g/l $^{15}NH_4Cl$ and 2 g/l ^{13}C-glucose), induced with 0.5 mM isopropyl β-D-thiogalactoside (IPTG) for 4–5 h. Protein purification was performed as follows: the cell pellet was disrupted by sonication in 20 mM Tris at pH 8.0. The supernatant was subjected to anion exchange (HiTrap Q HP column, Amersham Bioscience, NJ) and size exclusion (HiPrep 16/60 Sephacryl S-100 high resolution column, Amersham Bioscience, NJ) chromatography. Peak fractions were pooled and dialyzed three times against 2 l of distilled water, and finally against 1 l of MilliQ water. Pure protein was concentrated with Centriplus 3 kDa MWCO filters, and stored at −20°C before use. The protein was precipitated using a previously published protocol (Franks et al. 2005). In this study, we used the isotopically labeled sample diluted in 1:1 ratio with the natural abundance protein prior to precipitation. It should be noted that the dilution is not essential for the experiments presented in this work. Approximately 10 mg of sample (5 mg of U-^{13}C,^{15}N material) were center-packed between two cylindrical Vespel inserts into a 3.2 mm rotor. All experiments shown in this study were performed on a single sample.

NMR experiments

All experiments were performed on a Bruker Avance III spectrometer, operating at 600.130 MHz proton frequency, using a Bruker triple resonance ^{1}H–^{13}C–^{15}N 3.2 mm BioSolids MAS probe (Bruker USA, Billerica, MA). The spinning speed was 12 kHz, and the temperature of cooling gas was kept at 260 K in all experiments.

The pulse sequence for the ^{15}N detected ^{13}Cα–^{15}N (CAN) two-dimensional chemical shift correlation experiment is shown in Fig. 1a. It starts with ^{1}H/^{13}C cross-polarization (Pines et al. 1973) of 2 ms duration, with a radio-frequency (r.f.) field ramped around 68 kHz (10% ramp, optimized experimentally) on proton channel, and with a constant field of 54 kHz on ^{13}C channel. The ^{13}Cα/^{15}N band selective cross polarization (Baldus et al. 1998) was performed with an r.f. carbon field ramped around ~18 kHz (10% ramp), and with nitrogen r.f. field of 30 kHz. Proton CW decoupling during ^{13}Cα/^{15}N was set to 90 kHz. A proton field of 60 kHz was applied for SPINAL-64 (Fung et al. 2000) in the direct (^{15}N) dimension, whereas higher power SPINAL-64 decoupling of

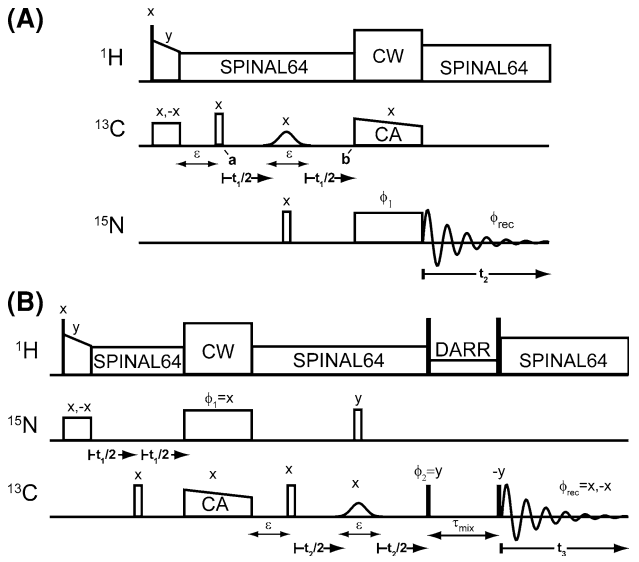

Fig. 1 Experimental pulse sequences. The filled and hollow bars represent $\pi/2$ and π-pulses. (**a**) A two-dimensional CAN chemical shift correlation experiment with homonuclear $J_{COC\alpha}$ decoupling in the indirect dimension is shown. Carbon carrier frequency is set in the aliphatic region, whereas the selective Gaussian π-pulse is applied off-resonance to the carbonyl region. The following phase cycling was used: ϕ_1, = (x, x, y, y, $-x$, $-x$, $-y$, $-y$), ϕ_{rec} = (x, $-x$, y, $-y$, $-x$, x, $-y$, y). The phase sensitive detection in t_1 dimension is accomplished using TPPI scheme, by incrementing the phase of the carbon ^{13}C–^{15}N CP pulse. (**b**) A three-dimensional NCACX correlation experiment with homonuclear J-decoupling is shown. A selective rotor-synchronized Gaussian π-pulse is applied off-resonance to the carbonyl region. The phase cycling is shown in the figure. The phase sensitive detection in t_1 and t_2 dimensions is accomplished using TPPI, by incrementing phases ϕ_1 and ϕ_2, respectively

80 kHz was used in the indirect (^{13}Cα) dimension. The proton $\pi/2$ pulse width was 2.7 μs, and the π-pulse widths for carbon and nitrogen were 10 and 12 μs, respectively. The ^{13}C carrier frequency was placed at 50 ppm for carbon chemical shift evolution in the t_1 dimension. The ^{15}N carrier frequency was placed at 117 ppm for nitrogen chemical shift evolution in the t_2 dimension. The Gaussian selective pulse was of 166.6 μs duration (2 rotor cycles), applied in the middle of the CO region (176 ppm). 240 real points were recorded in t_1 (^{13}Cα) dimension with an increment of 66 μs. 1024 complex points were recorded in the direct t_2 dimension, with the dwell time of 20 μs. 96 scans per point were acquired, with the recycling delay of 3 s, resulting in the total measurement time of 19.2 h.

The three-dimensional pulse sequence for the NCACX correlation is shown in Fig. 1b. It starts with ^{1}H/^{15}N cross-polarization (Pines et al. 1973) of 1 ms duration, with a radio-frequency field ramped around 68 kHz (10% ramp, optimized experimentally) on proton channel, and with a constant field of 54 kHz on ^{15}N channel. ^{15}N/^{13}Cα band selective cross polarization (Baldus et al. 1998) was performed with parameters similar to those in the CAN experiment. A proton field of 70 kHz was applied for SPINAL-64 decoupling in both direct and indirect evolution dimensions. Similar to the CAN experiment, the carrier frequency was placed at 117 and 50 ppm for nitrogen and carbon chemical shift evolution in t_1, and t_2/t_3 dimensions, respectively. The selective Gaussian pulse was applied in the middle of the carbonyl region. The frequency jump was implemented through phase modulation of the soft pulse. The ^{13}C–^{13}C mixing was accomplished using dipolar assisted rotational resonance (DARR) (Takegoshi et al. 2001) with r.f. field of 12 kHz applied to protons for 20 ms. The DARR mixing also works as a z-filter, and ensures that the transverse part of the magnetization, following the flip up pulse with phase ϕ_2 decays to zero. 64 real points were recorded in t_1 (^{15}N) dimension with an increment of 200 μs. 240 real points were recorded in t_2 (^{13}Cα) dimension with an increment of 66 μs. 1024 complex points were recorded in the direct t_3 dimension, with the dwell time of 20 μs. 2 scans per point were acquired, with the recycling delay of 3 s, resulting in the total measurement time of 26 h.

The CAN and NCACX experiments without J-decoupling (referred to as free precession experiments in the following (Igumenova et al. 2005)) were recorded using pulse sequences given in the Supporting Information. The acquisition parameters were identical to those given above for the J-decoupled experiments.

Data analysis

The carbon chemical shifts were indirectly referenced to 2,2-dimethyl-2-silapentane-5-sulfonic acid (DSS) through the ^{13}C adamantane downfield peak resonating at 40.48 ppm (Morcombe et al. 2003). The nitrogen chemical shifts were referenced indirectly by using the ratio of $\gamma_N/\gamma_C = 0.402979946$, taken without temperature factor correction, as recommended (Markley et al. 1998).

The data were processed with NMRPipe (Delaglio et al. 1995). The time domain data of the CAN experiment were zero filled to 2,048 × 8,192 complex points in $t_1 \times t_2$ dimensions. The time domain data of the NCACX experiment were zero filled to 1,024 × 2,048 × 4,096 complex points in $t_1 \times t_2 \times t_3$ dimensions. The data were Fourier transformed without using apodization function. Peaks were picked automatically in the 2D CAN and 3D NCACX spectra using scripts written in the CARA environment (Keller 2004). The assignments of cross peaks were based on previously published data (Franks et al. 2005). Although we have found that the peak positions were slightly shifted compared to the published assignments, the 2D NCA correlation patterns were found to be in a good agreement with the previously published data. Slight disagreements in peak positions may be explained by the

polymorphism of GB1 and its ability to crystallize in multiple forms, depending on the slight variation in crystallization conditions (Schmidt et al. 2007).

For the line width analysis, 1D slices along Cα dimensions were extracted and fitted with Gaussians using *Mathematica*. The quality of all fits was checked visually, but no attempts were made to estimate error bars for the extracted line widths. For 1D traces that could not be fitted reliably, the line widths were simply measured in the 1D extracted spectra at half peak height. Thus, the line widths quoted in the following are estimates only and are given for reference purposes.

Results and discussion

Effect of CO–Cα decoupling on the resolution of the backbone Cα sites

The simplest implementation of $J_{COC\alpha}$-decoupling in 2D MAS experiment is shown in Fig. 1a, where $^{13}C\alpha$–^{15}N 2D correlation is recorded with ^{15}N detection. The t_1 $^{13}C\alpha$ chemical shift evolution is taking place between points "**a**" and "**b**" in the pulse sequence. The selective Gaussian pulse of duration ε is applied to the carbonyl region in the middle of the t_1-evolution to refocus $J_{COC\alpha}$ interactions. The chemical shift evolution of the $^{13}C\alpha$ spins during the off-resonance pulse is refocused by an additional echo formed prior to the t_1 evolution (delay of the duration ε equal to the duration of the Gaussian pulse, and a hard π-pulse). Although this implementation leaves Cα–Cβ interactions intact, the most significant contributions to the Cα line widths coming from the CO–Cα J couplings are refocused.

Figure 2 shows a comparison of the free precession (a) and $J_{COC\alpha}$-decoupled (b) CAN spectra collected at a spinning frequency of 12 kHz. Both spectra were recorded under identical decoupling conditions and processed identically. Examination of the spectra reveals line narrowing for most of the resonances, as well as the improvement of their line shapes. A total of 33 cross peaks are resolved in the spectra, and their line shapes can be analyzed to demonstrate the resolution enhancement. We observed ~20 to 35 Hz improvement in the line width for the majority of the peaks, resulting from $J_{COC\alpha}$-decoupling. Representative one-dimensional slices taken through nitrogen dimension are shown in Fig. 3.

Free precession Cα resonances of Val29, Asp40, and Glu56 (upper row) have asymmetric line shapes, with visible splittings. In contrast, the decoupled resonances are much narrower, although some asymmetry still remains, probably due to $J_{C\alpha C\beta}$ couplings and second-order dipolar shifts (Igumenova et al. 2003).

Resolution enhancement in 3D NCACX spectroscopy

The CAN 2D spectra used above to demonstrate the advantages of J-decoupling are of limited applicability in the studies of large proteins. More realistic and useful are the 3D experiments, such as NCOCX, NCACX (Sun et al. 1997; Hong 1999; Rienstra et al. 2000), CONCA, CANCO, etc. (Franks et al. 2005). To demonstrate how $J_{COC\alpha}$-decoupling can be implemented in the context of a 3D experiment, we have recorded a 3D NCACX correlation spectrum using the pulse sequence shown in Fig. 1b. The implementation of the $J_{COC\alpha}$-decoupling here is similar to that used in the CAN experiment: the selective Gaussian pulse in the middle of the chemical shift evolution period is applied to the carbonyls and refocuses the J-interactions between CO and Cα spins, whereas the hard π-pulse on the ^{15}N channel refocuses the heteronuclear CN J-couplings. An additional delay of duration ε equal to the duration of the soft pulse, and the following hard π-pulse refocus the unwanted chemical shift evolution of the Cα spins, taking place during the off-resonance selective pulse.

Figure 4 shows representative 2D planes taken through the nitrogen dimension, and compares it with the result of the 3D NCACX experiment without J-decoupling. Figure 4a, b compare resolution enhancement for T51 and T53

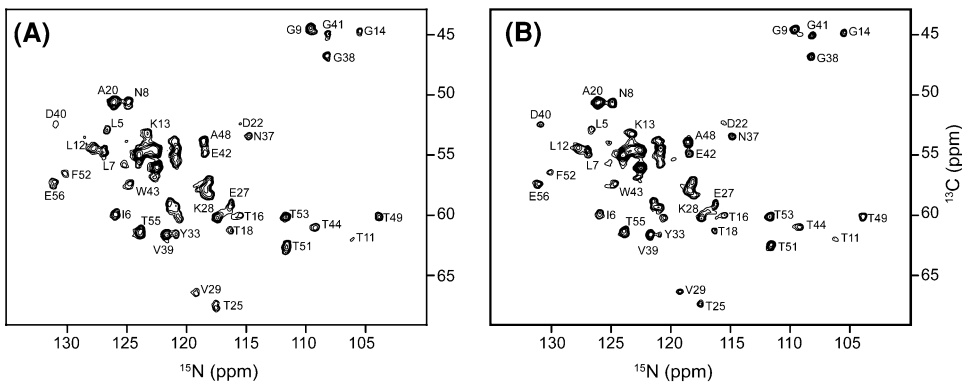

Fig. 2 Two-dimensional $^{13}C\alpha$–^{15}N free precession (**a**) and $J_{COC\alpha}$-decoupled (**b**) spectra. Both spectra were recorded at 600 MHz proton field and processed identically, as described in the text. The first contour was taken at 9 × σ (σ is the noise root-mean-square), with each additional contour level multiplied by 1.1

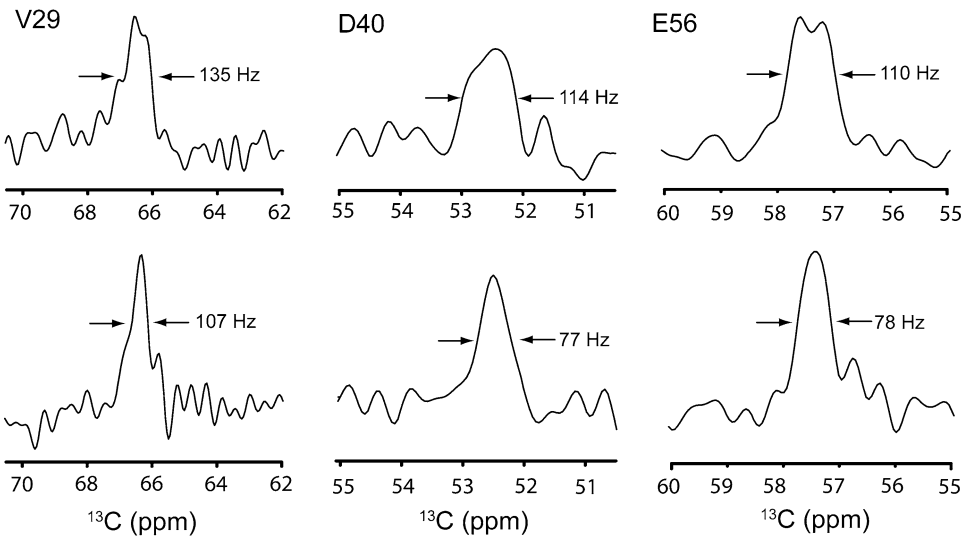

Fig. 3 Representative 1D traces extracted from the 2D CAN experiments. No apodization function was used in the data processing. Free precession 1D spectra are shown in the upper row. The corresponding J-decoupled spectra are shown in the lower row. All peaks are plotted on the same scale

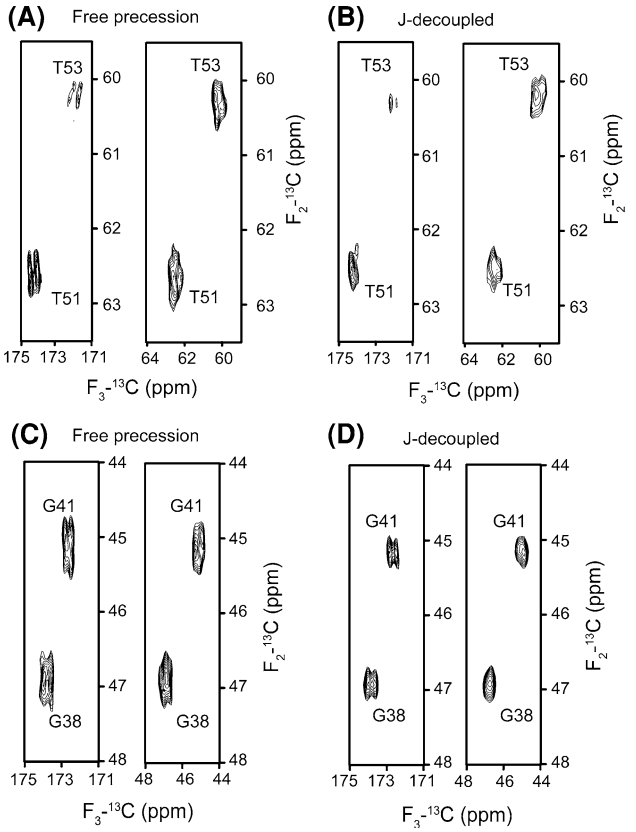

Fig. 4 2D ^{13}C–^{13}C planes extracted from the full 3D NCACX spectra. Pseudo-diagonal Cα–Cα peak and Cα–CO cross peaks are shown. (**a**, **b**): 2D planes taken through ^{15}N shift of 111.6 ppm for T51 and T53 residues are shown. (**c**, **d**) 2D planes taken through ^{15}N shift of 108.2 ppm for G38 and G41 are shown. The data were processed without apodization. For better visualization, the pseudo-diagonal and cross-peaks were normalized separately. The first contour levels were chosen at half intensity of T51 in (**a**) and (**b**), and at half intensity of G38 in (**c**) and (**d**)

residues. The line widths detected for these residues in the free precession experiment are 108 and 90 Hz, respectively. The application of the J-decoupling results in line narrowing for both lines: only moderate enhancement of 9 Hz was observed for T53 (width of 81 Hz was observed in the J-decoupled spectra), while T51 cross peak had a line width of 76 Hz, showing an enhancement of 32 Hz. Figure 4c, d compare free precession and J-decoupled 2D planes for two glycyl residues, G38 and G41. Glycines are unique among amino acids in a sense that they lack Cβ carbons, and their Cα resonances interact through bonds with carbonyls only. Thus, one can expect that the resolution enhancement resulting from J-decoupling would be larger for glycyl residues.

The line widths change from 133 to 74 Hz for G38, and from 133 to 89 Hz for G41. The other two glycyl residues exhibit similar improvements: from 95 to 62 Hz, and from 133 to 89 Hz for G9 and G14, respectively (results not shown). Further examples of 1D slices demonstrating the resolution enhancements are given in the Supporting information, and an overall comparison between the line widths observed in the free precession and J-decoupled experiments is shown in Fig. 5.

Overall, the resolution enhancements observed in the 3D NCACX experiment were similar to those of the CAN experiment, on the order of 20–35 Hz for most residues, with the largest enhancements observed for G14, G38, and G41.

The origin of the residual broadening was discussed previously (Igumenova et al. 2003). In addition to the obvious source—J-couplings between Cα and Cβ spins, the second-order dipolar shift affects the line shape significantly at moderate spinning frequencies. Much higher spinning frequencies, on the order of 105 ppm, are required to minimize these effects (Duma et al. 2003c).

Sensitivity considerations

The intensities of the cross-peaks in the J-decoupled spectra are determined by two major factors. There are

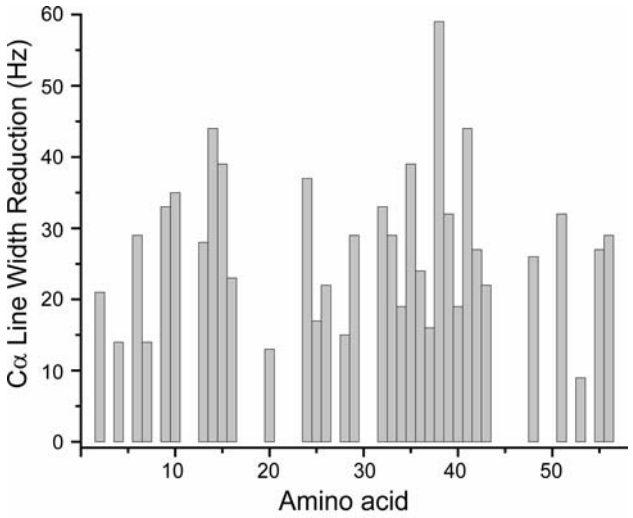

Fig. 5 Absolute reduction in the $^{13}C\alpha$ line width calculated as a difference between the free precession and J-decoupled spectra shown as a function of residue number. The line widths were estimated for well-resolved pseudo-diagonal N–CA–CA peaks

some signal losses associated with the transverse T_2' relaxation during the refocusing echo period, which consists of the delay ε and the off-resonance selective pulse. In a recent study, T_2' relaxation times were measured as a function of decoupling power and a spinning frequency for different nuclei (Chen et al. 2007). Under the decoupling and spinning frequency experimental conditions used in this work, the relaxation of Cα spins can be estimated to be on the order of 13 ms (Chen et al. 2007). With the total echo delay of 333 μs, and $T_2' \sim 13$ ms, the signal losses are estimated to be on the order of a few percent. The line width reduction, on the other hand, should result in sensitivity enhancement. To compare sensitivity of two experiments we used well-resolved cross-peaks in the N–CA–CO part of the spectrum. For the majority of peaks an enhancement on the order of 10–20% is observed. The overall sensitivity improvement was observed for most of the peaks, as can be seen in Table 1.

Conclusions

In summary, we demonstrated that the removal of Cα–CO homonuclear J-couplings results in the enhancement of spectral resolution. In this work, the $J_{COC\alpha}$-decoupling is demonstrated in the context of the 3D NCACX correlation experiment, and can be trivially extended to other experiments where Cα chemical shifts are recorder indirectly, for example to CANCO experiment (Franks et al. 2005). The J-decoupling is associated with minimal signal losses, and in combination with the line width reduction results in sensitivity enhancements.

Table 1 Signal-to-noise ratios for N–Cα–CO cross-peaks fully resolved in the 3D NCACX experiments in U-^{13}C,^{15}N GB1

N–Cα–CO cross-peak	Signal-to-noise ratio	
	Free precession	J-decoupled
Tyr3	7.1	7.2
Leu4	6.7	8.8
Ile6	7.2	7.5
Leu7	7.4	7.4
Asn8	6.7	7.6
Gly9	10.2	11.3
Lys13	7.6	9.4
Gly14	9.8	12.5
Glu15	6.7	7.4
Thr16	6.6	7.5
Ala20	6.4	7.2
Ala23	8.3	8.7
Ala24	6.7	8.9
Glu27	6.1	7.4
Lys28	6.9	6.7
Val29	6.5	6.1
Gln32	6.3	6.1
Tyr33	6.2	8.1
Ala34	6.5	10.9
Asp36	7.6	8.0
Asn37	6.6	9.6
Gly38	10.6	14.0
Gly41	9.6	13.5
Glu42	6.0	8.8
Tyr45	7.5	7.8
Thr51	8.2	9.4
Val54	7.4	7.9
Thr55	7.6	8.4
Glu56	8.9	9.1

Acknowledgements This research was supported by the University of Guelph (start-up funds to V.L.), the Natural Sciences and Engineering Research Council of Canada (DG250202 to L.S.B. and Grants RG298480-04 to V.L.), the Canada Foundation for Innovation, and the Ontario Innovation Trust. V.L. holds Canada Research Chair in Biophysics, and is a recipient of an Early Researcher Award from the Ontario Ministry of Research and Innovation. L.S. is a recipient of the Ontario Graduate Scholarship. M.A. is a recipient of a Doctoral Studentship from the Ministry of Higher Education and Scientific Research of Egypt.

References

Andrew ER, Bradbury A, Eades RG, Wynn VT (1963) Nuclear cross relaxation induced by specimen rotation. Phys Lett 4:99–100

Baldus M, Petkova AT, Herzfeld J, Griffin RG (1998) Cross polarization in the tilted frame: assignment and spectral simplification in heteronuclear spin systems. Mol Phys 95:1197–1207

Bruschweiler R, Griesinger C, Sorensen OW, Ernst RR (1988) Combined use of hard and soft pulses for omega-1 decoupling in two-dimensional NMR-spectroscopy. J Magn Reson 78:178–185

Chen L, Kaiser JM, Polenova T, Yang J, Rienstra CM, Mueller LJ (2007) Backbone assignments in solid-state proteins using J-based 3D heteronuclear correlation spectroscopy. J Am Chem Soc 129:10650–10651

Chevelkov V, Chen ZJ, Bermel W, Reif B (2005) Resolution enhancement in MAS solid-state NMR by application of C-13 homonuclear scalar decoupling during acquisition. J Magn Reson 172:56–62

Delaglio F, Grzesiek S, Vuister GW, Zhu G, Pfeifer J, Bax A (1995) NMRPipe - a multidimensional spectral processing system based on UNIX pipes. J Biomol NMR 6:277–293

Duma L Hediger S, Brutscher B, Bockmann A, Emsley L (2003a) Resolution enhancement in multidimensional solid-state NMR spectroscopy of proteins using spin-state selection. J Am Chem Soc 125:11816–11817

Duma L, Hediger S, Lesage A, Emsley L (2003b) Spin-state selection in solid-state NMR. J Magn Reson 164:187–195

Duma L, Hediger S, Lesage A, Sakellariou D, Emsley L (2003c) Carbon-13 lineshapes in solid-state NMR of labeled compounds. Effects of coherent CSA-dipolar cross-correlation. J Magn Reson 162:90–101

Franks WT, Zhou DH, Wylie BJ, Money BG, Graesser DT, Frericks HL, Sahota G, Rienstra CM (2005) Magic-angle spinning solid-state NMR spectroscopy of the beta 1 immunoglobulin binding domain of protein G (GB1): N-15 and C-13 chemical shift assignments and conformational analysis. J Am Chem Soc 127:12291–12305

Fung BM, Khitrin AK, Ermolaev K (2000) An improved broadband decoupling sequence for liquid crystals and solids. J Magn Reson 142:97–101

Hiller M, Krabben L, Vinothkumar KR, Castellani F, van Rossum BJ, Kuhlbrandt W, Oschkinat H (2005) Solid-state magic-angle spinning NMR of outer-membrane protein G from *Escherichia coli*. Chembiochem 6:1679–1684

Hong M (1999) Resonance assignment of C-13/N-15 labeled solid proteins by two- and three-dimensional magic-angle-spinning NMR. J Biomol NMR 15:1–14

Igumenova TI, McDermott AE (2003) Improvement of resolution in solid state NMR spectra with J-decoupling: an analysis of lineshape contributions in uniformly C-13-enriched amino acids and proteins. J Magn Reson 164:270–285

Igumenova TI, McDermott AE (2005) Homo-nuclear C-13 J-decoupling in uniformly C-13-enriched solid proteins. J Magn Reson 175:11–20

Jaroniec CP, MacPhee CE, Astrof NS, Dobson CM, Griffin RG (2002) Molecular conformation of a peptide fragment of transthyretin in an amyloid fibril. Proc Natl Acad Sci USA 99:16748–16753

Keller R (2004) The computer aided resonance assignment tutorial, first ed. CANTINA Verlag Goldau

Levitt MH, Raleigh DP, Creuzet F, Griffin RG (1990) Theory and simulations of homonuclear spin pair systems in rotating solids. J Chem Phys 92:6347–6364

Li Y, Wylie BJ, Rienstra CM (2006) Selective refocusing pulses in magic-angle spinning NMR: characterization and applications to multi-dimensional protein spectroscopy. J Magn Reson 179: 206–216

Lorch M, Fahem S, Kaiser C, Weber I, Mason AJ, Bowie JU, Glaubitz C (2005) How to prepare membrane proteins for solid-state NMR: a case study on the α-helical integral membrane protein diacylglycerol kinase from *E. coli*. Chembiochem 6:1693–1700

Markley JL, Bax A, Arata Y, Hilbers CW, Kaptein R, Sykes BD, Wright PE, Wuthrich K (1998) Recommendations for the presentation of NMR structures of proteins and nucleic acids - IUPAC-IUBMB-IUPAB inter-union task group on the standardization of data bases of protein and nucleic acid structures determined by NMR spectroscopy. Eur J Biochem 256:1–15

Martin RW, Zilm KW (2003) Preparation of protein nanocrystals and their characterization by solid state NMR. J Magn Reson 165:162–174

Morcombe CR, Zilm KW (2003) Chemical shift referencing in MAS solid state NMR. J Magn Reson 162:479–486

Paravastu AK, Petkova AT, Tycko R (2006) Polymorphic fibril formation by residues 10-40 of the Alzheimer's beta-amyloid peptide. Biophys J 90:4618–4629

Pauli J, van Rossum B, Forster H, de Groot HJM, Oschkinat H (2000) Sample optimization and identification of signal patterns of amino acid side chains in 2D RFDR spectra of the alpha-spectrin SH3 domain. J Magn Reson 143:411–416

Pines A, Gibby MG, Waugh JS (1973) Proton-enhanced NMR of dilute spins in solids. J Chem Phys 59:569–590

Rienstra CM, Hohwy M, Hong M, Griffin RG (2000) 2D and 3D N-15-C-13-C-13 NMR chemical shift correlation spectroscopy of solids: assignment of MAS spectra of peptides. J Am Chem Soc 122:10979–10990

Schmidt HL, Sperling LJ, Gao YG, Wylie BJ, Boettcher JM, Wilson SR, Rienstra CM (2007) Crystal polymorphism of protein GB1 examined by solid-state NMR spectroscopy and X-ray diffraction. J Phys Chem B 111:14362–14369

Siemer AB, Ritter C, Ernst M, Riek R, Meier BH (2005) High-resolution solid-state NMR spectroscopy of the prion protein HET-s in its amyloid conformation. Angewandte Chemie-International Edition 44:2441–2444

Straus SK, Bremi T, Ernst RR (1996) Resolution enhancement by homonuclear J decoupling in solid-state MAS NMR. Chem Phys Lett 262:709–715

Straus SK, Bremi T, Ernst RR (1998) Experiments and strategies for the assignment of fully C-13/N-15-labelled polypeptides by solid state NMR. J Biomol NMR 12:39–50

Sun BQ, Rienstra CM, Costa PR, Williamson JR, Griffin RG (1997) 3D N-15-C-13-C-13 chemical shift correlation spectroscopy in rotating solids. J Am Chem Soc 119:8540–8546

Takegoshi K, Nakamura S, Terao T (2001) C-13-H-1 dipolar-assisted rotational resonance in magic-angle spinning NMR. Chem Phys Lett 344:631–637

Wylie BJ, Sperling LJ, Rienstra CM (2008) Isotropic chemical shifts in magic-angle spinning NMR spectra of proteins. Phys Chem Chem Phys 10:405–413

Zhong L, Bamm VV, Ahmed MA, Harauz G, Ladizhansky V (2007) Solid-state NMR spectroscopy of 18.5 kDa myelin basic protein reconstituted with lipid vesicles: spectroscopic characterisation and spectral assignments of solvent-exposed protein fragments. Biochim Biophys Acta 1768:3193–3205

Zhou DHH, Kloepper KD, Winter KA, Rienstra CM (2006) Band-selective C-13 homonuclear 3D spectroscopy for solid proteins at high field with rotor-synchronized soft pulses. J Biomol NMR 34:245–257